THE JOURNAL OF BIOLOGICAL CHEMISTRY VOL. 283, NO. 51, pp. 35724–35734, December 19, 2008

Gain-of-function R225Q Mutation in AMP-activated Protein Kinase γ3 Subunit Increases Mitochondrial Biogenesis in Glycolytic Skeletal Muscle*

Received for publication, July 3, 2008, and in revised form, September 24, 2008 Published, JBC Papers in Press, October 6, 2008, DOI 10.1074/jbc.M805078200

Pablo M. Garcia-Roves, Megan E. Osler, Maria H. Holmström, and Juleen R. Zierath[1]

From the Department of Molecular Medicine and Surgery, Section Integrative Physiology, Karolinska Institutet, von Eulers Väg 4, 4th Floor, S-171 77 Stockholm, Sweden

AMP-activated protein kinase (AMPK) is a heterotrimeric complex, composed of a catalytic subunit (α) and two regulatory subunits (β and γ), that works as a cellular energy sensor. The existence of multiple heterotrimeric complexes provides a molecular basis for the multiple roles of this highly conserved signaling system. The AMPK γ3 subunit is predominantly expressed in skeletal muscle, mostly in type II glycolytic fiber types. We determined whether the AMPK γ3 subunit has a role in signaling pathways that mediate mitochondrial biogenesis in skeletal muscle. We provide evidence that overexpression or ablation of the AMPK γ3 subunit does not appear to play a critical role in defining mitochondrial content in resting skeletal muscle. However, overexpression of a mutant form (R225Q) of the AMPK γ3 subunit (Tg-AMPKγ3^{225Q}) increases mitochondrial biogenesis in glycolytic skeletal muscle. These adaptations are associated with an increase in expression of the co-activator PGC-1α and several transcription factors that regulate mitochondrial biogenesis, including NRF-1, NRF-2, and TFAM. Succinate dehydrogenase staining, a marker of the oxidative profile of individual fibers, was also increased in transversal skeletal muscle sections of white gastrocnemius muscle from Tg-AMPKγ3^{225Q} mice, independent of changes in fiber type composition. In conclusion, a single nucleotide mutation (R225Q) in the AMPK γ3 subunit is associated with mitochondrial biogenesis in glycolytic skeletal muscle, concomitant with increased expression of the co-activator PGC-1α and several transcription factors that regulate mitochondrial proteins, without altering fiber type composition.

Skeletal muscle is a heterogeneous tissue that is composed of different fiber types, which are characterized by distinct contractile and metabolic properties. Skeletal muscle adapts to different conditions that require quick or long term alterations in power, force production, or substrate availability and utilization. Regular endurance exercise training promotes mitochondrial biogenesis (1) through an orchestrated change in the expression of genes that encode mitochondrial proteins (2). The AMPK[2] pathway plays a major role in the physiological regulation of mitochondrial function and biogenesis (3–8) and has been suggested to prevent or reverse peripheral insulin resistance associated with Type 2 diabetes (9–11).

AMPK is a cellular energy sensor that is activated in response to an increase in the AMP/ATP ratio. Once activated, AMPK coordinates signaling events to initiate catabolic processes that increase energy production and terminate anabolic processes, such as protein synthesis. AMPK activation modulates transcription of specific genes involved in energy metabolism, thereby exerting long term metabolic control. AMPK exists as a heterotrimeric complex composed of a catalytic (α) and two regulatory (β and γ) subunits. The α- and β-subunits are each encoded by two genes (α1, α2, β1, and β2), and the γ subunit is encoded by three genes (γ1, γ2, and γ3), yielding 12 possible heterotrimeric complexes. In human skeletal muscle, only three (α1β2γ1, α2β2γ1, and α2β2γ3) of the 12 AMPK complexes are present (12). The existence of multiple heterotrimeric complexes provides a molecular basis for the multiple roles of this highly conserved signaling system in nutrient regulation and utilization in mammalian cells (13).

Exercise activates AMPK (11) and induces skeletal muscle mitochondrial biogenesis (14), but the mechanism is incompletely resolved. Molecular approaches using transgenic or knock-out technology that targets AMPK subunit isoforms provide direct evidence for specific signal transducers in mediating mitochondrial biogenesis. The AMPK γ3 subunit is predominantly expressed in glycolytic skeletal muscle (15–20). Transgenic expression of the R225Q mutation in mice (Tg-AMPKγ3^{225Q} mice) is associated with increased skeletal muscle glycogen content, fatigue resistance, and protection from diet-induced insulin resistance through increased β-oxidation (17). These metabolic responses in sedentary Tg-AMPKγ3^{225Q} mimic the effects of exercise training and are partly mediated through transcriptional regulation of genes important for glycolytic and oxidative metabolism (20). However, the role of the AMPK γ3 subunit, as well as whether mutations in this isoform regulate mitochondrial biogenesis and function in resting skeletal muscle, is unresolved.

* This work was supported by the European Foundation for the Study of Diabetes, Swedish Research Council, Swedish Diabetes Association, Strategic Research Foundation (INGVAR II and Center for Functional Genetics), Knut and Alice Wallenberg Foundation, Novo Nordisk Research Foundation, Research and Education, Karolinska University Hospital, and Commission of the European Communities Contract LSHM-CT-2004-005272 EXGENESIS and Contract LSHM-CT-2004-512013 EUGENE2. The costs of publication of this article were defrayed in part by the payment of page charges. This article must therefore be hereby marked "*advertisement*" in accordance with 18 U.S.C. Section 1734 solely to indicate this fact.

[1] To whom correspondence should be addressed. Tel.: 46-8-5248-7581; Fax: 46-8-33-54-36; E-mail: Juleen.Zierath@ki.se.

[2] The abbreviations used are: AMPK, AMP-activated protein kinase; mtDNA, mitochondrial DNA; EDL, extensor digitorum longus; MES, 4-morpholineethanesulfonic acid; WT, wild type; MyHC, myosin heavy chain.

Here we determined the role of the AMPK γ3 subunit in the regulation of mitochondrial function and biogenesis in glycolytic skeletal muscle. Three mouse models were used to genetically dissect the functional role of the AMPKγ3 isoform: transgenic mice overexpressing either the wild-type or the R225Q mutant subunit (Tg-AMPKγ3^{wt} or Tg-AMPKγ3^{225Q}) and knock-out mice (AMPKγ3$^{-/-}$). We provide evidence that the mutant form of the AMPK γ3 subunit influences gene expression, promoting adaptive metabolic responses on mitochondrial function and biogenesis in skeletal muscle. Therefore, the AMPK γ3 subunit may play a critical role in mediating the metabolic adaptations in glycolytic skeletal muscle in response to cellular stress and energy deficiency.

EXPERIMENTAL PROCEDURES

Reagents for denaturing electrophoresis (SDS-PAGE) and Western blot analysis were from Bio-Rad. Reagents for enhanced chemiluminescence (ECL) were purchased from Amersham Biosciences. Mouse anti-human monoclonal antibodies against NADH ubiquinol oxidoreductase 39-kDa subunit (Complex I), succinate-ubiquinol oxidoreductase 70-kDa subunit (Complex II), ubiqinol-cytochrome *c* oxidoreductase subunits I (Complex III), cytochrome oxidase subunit I (Complex IV), and ATP synthase subunit α were obtained from Molecular Probes, Inc. (Eugene, OR). Mouse anti-cytochrome *c* monoclonal antibody was purchased from PharMingen International (San Diego, CA). Polyclonal rabbit anti-human UCP-3 (uncoupling protein 3) and anti-mouse PGC-1 (peroxisome proliferator γ co-activator-1) antibodies were purchased from Chemicon International (Temecula, CA). Polyclonal goat anti-mouse NRF-1 (nuclear respiratory factor 1) and TFAM (mitochondrial transcription factor A) were purchased from Santa Cruz Biotechnology, Inc. (Santa Cruz, CA). Horseradish peroxidase-conjugated donkey anti-rabbit, donkey anti-goat, and goat anti-mouse IgG were purchased from Jackson ImmunoResearch Laboratories (West Grove, PA). Rat IgG was obtained from Santa Cruz Biotechnology. Myosin heavy chain (MyHC) type IIa (SC-71) and MyHC type I (D-5) antibodies were kindly donated by Professor Stefano Schiaffino. TRIzol reagent for isolation of RNA was purchased from Invitrogen. Reagents for isolation of mRNA were obtained from Ambion (Austin, TX). TaqMan reverse transcription and RT-PCR reagents were purchased from Applied Biosystems (Foster City, CA). All other reagents were obtained from Sigma.

Animal Care—This research was approved by the regional animal ethical committee. Animals were maintained in a temperature- and light-controlled environment and were cared for in accordance with regulations for the protection of laboratory animals. Animals were maintained under a 12-h light/dark cycle and had free access to water and standard rodent chow. Three different mouse models were used to investigate the role of the skeletal muscle specific AMPK γ3 subunit in the regulation of mitochondrial function and mitochondrial biogenesis: AMPK γ3 knock-out (AMPKγ3$^{-/-}$), AMPK γ3 wild-type transgenic (Tg-AMPKγ3^{wt}), and AMPK γ3R225Q transgenic (Tg-AMPKγ3^{225Q}). The mouse models used in this study have been described previously (17). The AMPKγ3$^{-/-}$ mice were created by conventional gene targeting techniques. Tg-AMPKγ3^{wt} and Tg-AMPKγ3^{225Q} mice express the wild-type γ3 subunit or the R225Q mutant γ3 subunit under the control of mouse myosin-light chain promoter and enhancer elements. All three models used in the study were bred into a C57BL/6 genetic background. Transgenic mice were compared with nontransgenic littermates. Knock-out homozygote mice were compared with homozygous wild-type littermates. In our initial characterization of these models (17), we reported a marked overexpression of the wild-type transgene in extensor digitorum longus (EDL), gastrocnemius, and quadriceps muscle (~16.5-, 6.6-, and 1.7-fold, respectively), but no overexpression or only a moderate overexpression of the mutant transgene (~0.7-, 1.0-, and 1.8-fold, respectively). The differences in the level of expression between the two transgenic mice may be explained by positional effects or number of integrated copies. We also reported that the levels of endogenous AMPKγ3 transcript in Tg-AMPKγ3^{225Q} mice tended to be decreased (17). Furthermore, the amount of expressed γ3 protein, as well as α, β, or the other γ subunits, was unchanged, in the Tg-AMPKγ3^{225Q} mice (17). Thus, AMPK expression in Tg-AMPKγ3^{225Q} mice appears to resemble the expression pattern in nontransgenic wild-type mice, both in regard to tissue distribution and protein expression. The mutant form (R225Q) presumably replaced endogenous γ3, based on the relative mRNA expression (17). However, endogenous and exogenous forms of the protein, as assessed by Western blot analysis, were indistinguishable (17), since they differed by a single amino acid substitution. Mice were anesthetized with an intraperitoneal injection of Avertin (2,2,2-tribromoethanol (99%) and tertiary amyl alcohol (0.015–0.017 ml/g body weight), intraperitoneally), and the white portion of the gastrocnemius muscle was dissected and cleaned of fat and blood and snap-frozen in liquid nitrogen.

Quantitative PCR—Quantification of mRNA was performed using real-time PCR as described (18). Total RNA isolated from the white portion of the gastrocnemius muscle was reverse transcribed with oligo(dT) primers using the SuperScript First Strand Synthesis System (Invitrogen). Reactions were performed in duplicate in a 96-well format using a Prism 7000 Sequence Detector and fluorescence-based SYBR-green technology (Applied Biosystems). Mouse-specific primer/probe sets used to detect specific gene expression were selected by using PRIMER EXPRESS (Applied Biosystems) and are available upon request. The following primers for detection of the different myosin heavy chain isoforms were used: MyHC I forward (TTGTGCTACCCAGCTCTAAGGG) and reverse (CTGCTTCCACCTAAAGGGCTG); MyHC IIa forward (AAGCGAAGAGTAAGGCTGTC) and reverse (CTTGCAAAGGAACTTGGGCTC); MyHC IIb forward (GAAGAGCCGAGAGGTTCACAC) and reverse (CAGGACAGTGACAAAGAACGTC); and MyHC IIx forward (GAAGAGTGATTGATCCAAGTG) and reverse (TATCTCCCAAAGTTATGAGTACA). Relative quantities of target transcripts were calculated after normalization against a housekeeping gene (acidic ribosomal phosphoprotein PO) using the relative standard curve method.

Muscle Lysate Preparation and Western Blot Analysis—White gastrocnemius muscles were homogenized in ice-cold buffer (10% (v/v) glycerol, 20 mM sodium pyrophosphate, 150

mM NaCl, 50 mM HEPES (pH 7.5), 1% Nonidet P-40, 20 mM β-glycerophosphate, 10 mM sodium fluoride, 1 mM EDTA, 1 mM EGTA, 2 mM phenylmethylsulfonyl fluoride, 10 μg/ml aprotinin, 10 μg/ml leupeptin, 2 mM sodium orthovanadate, and 3 mM benzamidine (pH 7.4)). Whole muscle homogenates were rotated end-over-end for 1 h at 4 °C and then subjected to three freeze and thaw cycles to disrupt the mitochondria. The homogenates were centrifuged at 10,000 × *g* for 15 min at 4 °C, and the supernatant was collected. Protein concentration was measured using a BCA protein assay kit, and sample dilutions were adjusted to yield equal protein concentration. Aliquots for Western blot analysis were mixed with Laemmli buffer, separated by SDS-PAGE, and transferred to polyvinylidene difluoride membranes. The membranes were blocked overnight at 4 °C with 5% nonfat dry milk in Tris-buffered saline containing 0.1% (v/v) Tween. The blots were probed with primary antibody, followed by incubation with the appropriate horseradish peroxidase-conjugated anti-IgG antibody. Antibody-bound protein was detected using enhanced chemiluminescence and quantified by densitometry.

Quantification of Mitochondrial DNA Copy Number—To determine mitochondrial DNA levels, total genomic DNA was isolated from white gastrocnemius, and the amount of mitochondrial DNA (mtDNA) was compared with nuclear DNA. Primers for mtDNA (cytochrome b; forward, AAAGCCACCTTGACCCGATT; reverse, GATTCGTAGGGCCGCGATA; Custom TaqMan® TAMRA™ probe, CGCTTTCCACTTCATCTTACCATT), nuclear DNA (mouse β-actin), and 1× TaqMan Universal PCR Master Mix were supplied by Applied Biosystems. Real time PCR quantitative analysis was performed using ΔCT on the sequence detector system ABI-Prism 7000. Copy number of mtDNA and nuclear DNA was calculated using the threshold cycle number (C_T) intrapolated from the standard curve.

Histological Methods—Gastrocnemius, plantaris, soleus, and EDL muscles were harvested and frozen together in Tissue-Tek® O.C.T.™ compound (Tissue-Tek, Sakura Finetek Europe, Zoeterwoude, Netherlands). Serial skeletal muscle cross-sections (10 μm for fiber type measurement, immunostaining, and succinate dehydrogenase (SDH) staining) were generated in a Microstat HM 500M cryostat, mounted on SuperFrost slides (Menzel GmbH & Co., Braunschweig, Germany) and stored at −20 °C until use. Skeletal muscle fiber type (I, IIa, and IIb) was quantified using myosin ATPase staining (21). Sections were subjected to acidic preincubation (0.2 M sodium acetate, 0.1 M KCl, pH 4.43), incubated with ATP (90 mM glycine, 65 mM $CaCl_2$, 90 mM NaCl, 3 mM ATP, pH 9.4), and subsequently treated with 1% (w/v) $CaCl_2$, 2% (w/v) $CoCl_2$, and 1% (v/v) $(NH_4)_2S$. Immunostaining was performed with MyHC type IIa (SC-71) and MyHC type I (D-5) antibodies, as directed by the M.O.M.™ kit (Vector Laboratories, Burlingame, CA). SDH staining was performed by treatment with incubation solution (6.5 mM NaH_2PO_4, 43.5 mM Na_2HPO_4, 0.6 mM nitro blue tetrazolium, and 50 mM sodium succinate, pH 7.6), followed by treatment with physiological saline and 15% ethanol. Following histological procedures, coverslips were secured over the slides with aqueous mounting medium (Dako, Glostrup, Denmark).

Image Capture and Analysis—Images for fiber type analysis were captured using an Olympus DP70 camera (Olympus Corp., Japan) and Cast software (Visiopharm, Horsholm, Denmark). Quantification of the fiber type composition was performed using Image J version 1.37 (National Institutes of Health). Fiber type identification was made using threshold values of particle density: type I fibers ≤40, type IIa ≤210, and type IIb ≥210. An average of 100 fibers/muscle was counted, and the percentage of each fiber type per muscle was calculated.

Electrophoretic Separation of MyHC Isoforms—White gastrocnemius muscle was dissected and homogenized in lysis buffer (137 mM NaCl, 2.7 mM KCl, 1 mM $MgCl_2$, 0.5 mM Na_3VO_4, 1% (v/v) Triton X-100, 10% (v/v) glycerol, 20 mM Tris (pH 7.8), 1 μg/ml leupeptin, 1 mM phenylmethylsulfonyl fluoride, 10 mM NaF, 1 μg/ml aprotinin, 1 mM EDTA, 5 mM pyrophosphate, and 1 μM microcystin), and 50 μl was removed prior to centrifugation. Total protein content was assessed using a BCA assay. Electrophoretic separation of MyHC isoforms was performed as described (22). Whole muscle homogenate was separated on a glycerol SDS-polyacrylamide gel (stacking gel: 4% (v/v) acrylamide (40:1), 0.8% (v/v) bis (2:1), and 37% (v/v) glycerol; resolving gel: 8% (v/v) acrylamide (40:1), 0.2% (v/v) bis (2:1), and 37% (v/v) glycerol). Gels were run using a Minigel system (Bio-Rad) at 4 °C, 160 V for 28 h (5–10 mA) with upper and lower running buffer (100 mM Tris base, 150 mM glycine, 0.1% (w/v) SDS, pH 8.6; and 50 mM Tris base, 75 mM glycine, 0.05% SDS, respectively) at equal surface level. Gels were fixed overnight in 10% acetic acid and 40% ethanol and stained using the SilverQuest™ silver staining kit (Invitrogen). Images for quantification were acquired by scanning the gels with a GS-710 calibrated imaging densitometer (Bio-Rad), and the relative proportion of each MyHC isoform was determined using Quantity 1 software (Bio-Rad). Bands were identified according to their migration characteristics, as described (22).

Electron Microscopy—For ultrastructural examination, white gastrocnemius muscle samples were processed for electron microscopic analysis. Skeletal muscle from Tg-AMPKγ3^{225Q} mice and nontransgenic littermates was perfused-fixed with 2.5% glutaraldehyde with 300 mM sucrose in 0.1 M cacodylate buffer, pH 7.2–7.4, dissected, cut into 1 × 1 × 2-mm pieces, and fixed overnight. Samples were postfixed for 1 h in 1% (v/v) osmium tetroxide, dehydrated through a graded series of alcohol/acetone, and embedded in Fluka Durcupan resin. Ultrathin 70-nm sections were placed on copper mesh grids (EMS), counterstained with uranyl acetate and lead citrate, and examined with a Morgagni 268 transmission electron microscope (FEI Co., Hillsboro, OR). For quantification of percentage area of mitochondria 10 random images/muscle were captured using an AMT camera system (Advance Microscopy Techniques Corp., Danvers, MA) at ×20,400. Total mitochondrial volume density, and number was determined.

Mitochondrial Respiration—Mitochondrial function was assessed using respirometry (Oroboros Oxygraph-2k; Oroboros Instruments, Innsbruck, Austria), as previously described (23, 24). White gastrocnemius muscle was placed in a relaxing solution (2.8 mM Ca_2K_2EGTA, 7.2 mM K_2EGTA, 5.8 mM ATP, 6.6 mM $MgCl_2$, 20 mM taurine, 15 mM sodium phosphocreatine, 20 mM imidazole, 0.5 mM dithiothreitol, and 50 mM MES, pH

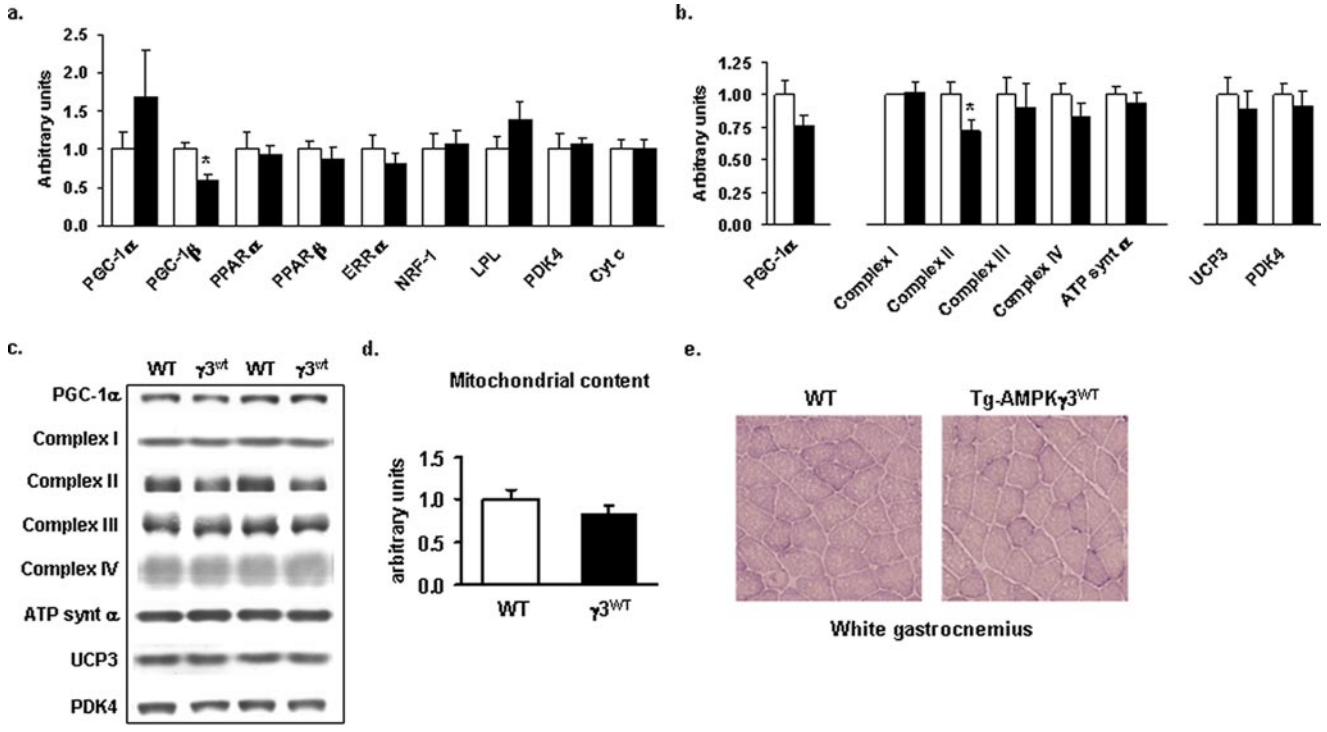

FIGURE 1. **Skeletal muscle mitochondrial content is unaltered by AMPK γ3 subunit overexpression.** *a*, mRNA content of different transcription factors responsible for mitochondrial biogenesis regulation and different mitochondrial markers in AMPK γ3 subunit transgenic (Tg-AMPKγ3^{wt}) mice ($n = 7$) *versus* nontransgenic (WT) littermates ($n = 7$). *b*, Protein content of factors involved in mitochondrial biogenesis in Tg-AMPKγ3^{wt} mice ($n = 8$) and WT nontransgenic littermates ($n = 7$). *c*, representative immunoblots for the different proteins represented in Fig. 1*b*. *d*, mitochondrial content in gastrocnemius muscle from Tg-AMPKγ3^{wt} mice ($n = 7$) and nontransgenic littermates ($n = 7$). Mitochondrial content was estimated as the ratio between copy numbers of mtDNA (cytochrome *b*) *versus* nuclear DNA (β-actin). *e*, representative SDH activity in tranversal sections of white gastrocnemius muscle from Tg-AMPKγ3^{wt} mice ($n = 4$) and nontransgenic littermates ($n = 4$). Data are represented as mean ± S.E. -fold change with respect to the corresponding nontransgenic littermates. *Open bar*, nontransgenic WT; *closed bar*, Tg-AMPKγ3^{wt}. *, $p < 0.05$; significantly different from nontransgenic WT mice.

7.1), and fibers were gently separated under a microscope using fine forceps. Following permeabilization of the sarcolemma in 0.005% (w/v) saponin, the tissue was equilibrated in ice-cold respirometry medium (0.5 mM EGTA, 3 mM $MgCl_2$, 60 mM potassium lactobionate, 20 mM taurine, 10 mM KH_2PO_4, 20 mM HEPES, 110 mM sucrose, and 0.1% (w/v) bovine serum albumin, pH 7.1) and blotted, and ~1.5–2 mg of tissue/chamber was weighed and used for the experiment. All measurements were made in duplicate. Basal O_2 flux from complex I (*CI* in Fig. 6) of the respiratory chain was measured by adding the substrates malate (final concentration 1.6 mM), glutamate (20 mM), and pyruvate (9.8 mM). Oxidative phosphorylation was quantified by the addition of ADP (4.8 mM), followed by the complex II substrate succinate (9.6 mM), for convergent electron flow through Complexes I + II. Then the protonophore carbonyl-cyanide-4-(trifluoromethoxy)-phenylhydrazone (0.2 μM) was titrated to achieve maximum flux trough the electron transfer system. Finally, electron transport through complexes I and III was inhibited by the sequential addition of rotenone (0.1 μM) and antimycin A (2.4 μM), respectively. The oxygen flux obtained in each step of the protocol was normalized by mitochondrial content/nuclei as determined in the same muscle using mitochondrial/nuclear DNA ratio (protocol detailed above).

Statistical Analysis—Values are expressed as mean ± S.E. Statistically significant differences were determined using unpaired Student's *t* tests.

RESULTS

Skeletal Muscle Mitochondrial Content Is Unaltered in Tg-AMPKγ3^{wt} Mice—To ascertain whether overexpression of the AMPK γ3 subunit is sufficient to induce skeletal muscle mitochondrial biogenesis, we studied sedentary mice overexpressing the wild-type form of the AMPK γ3 subunit in glycolytic muscle (Tg-AMPKγ3^{wt}). The mRNA expression profile of different transcription factors and mitochondrial markers was unaltered between Tg-AMPKγ3^{wt} mice and nontransgenic littermates (Fig. 1*a*). However, mRNA expression of the co-activator PGC-1β was reduced in skeletal muscle from Tg-AMPKγ3^{wt} mice. Protein content of several transcription factors, markers of the different complexes of the respiratory chain, and pyruvate dehydrogenase kinase 4 (PDK4), a key enzyme in the regulation of substrate utilization and the switch between glucose and fatty acid oxidation, was unaltered between Tg-AMPKγ3^{wt} mice and nontransgenic littermates (Fig. 1, *b* and *c*). However, protein content of SDH ubiquinol oxidoreductase (complex II of the respiratory chain) was reduced in skeletal muscle from Tg-AMPKγ3^{wt} mice (Fig. 1, *b* and *c*). Muscle mitochondrial content and transverse sections showing succinate dehydrogenase activity (SDH) were similar between Tg-AMPKγ3^{wt} mice and nontransgenic littermates (Fig. 1, *d* and *e*). Thus, our results provide evidence to suggest that increasing the amount of the AMPK γ3 subunit is insufficient to induce mitochondrial adaptations in sedentary mice.

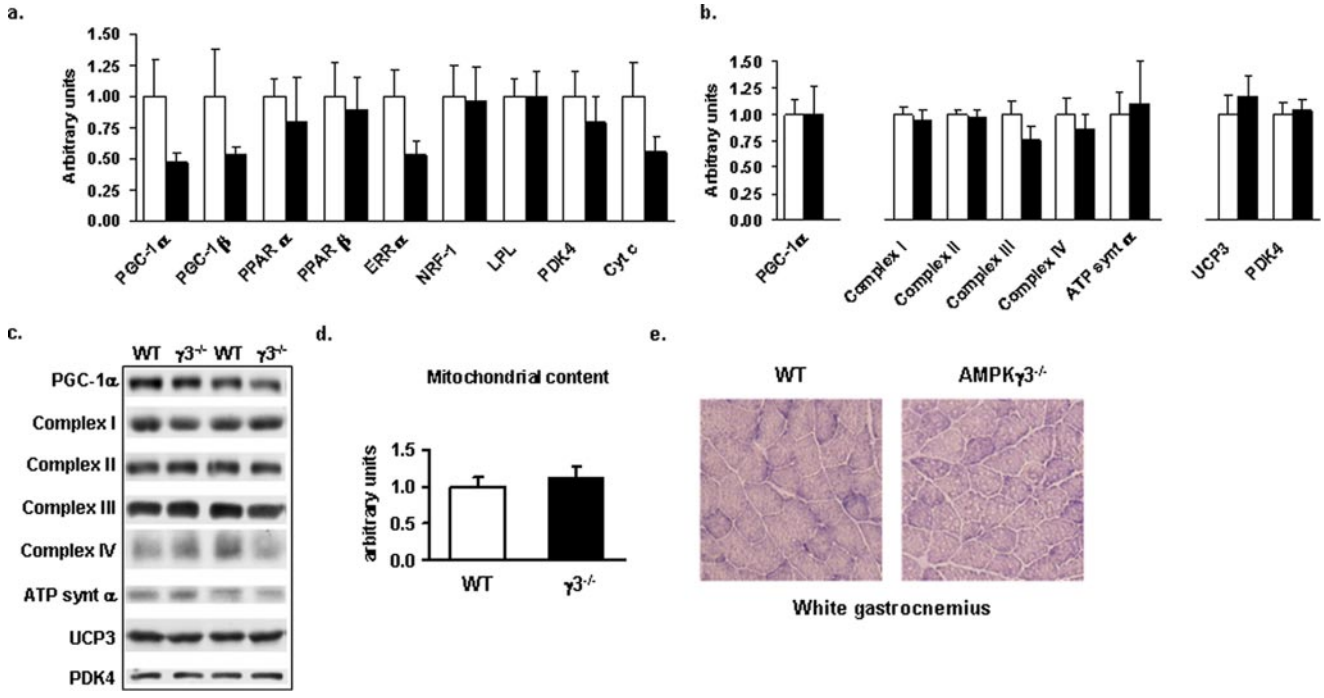

FIGURE 2. **Skeletal muscle mitochondrial content is unaltered in AMPK γ3 knock-out (AMPKγ3$^{-/-}$) mice.** *a*, mRNA content of different transcription factors responsible for mitochondrial biogenesis regulation and different mitochondrial markers in AMPKγ3$^{-/-}$ mice ($n = 7$) and homozygous WT littermates ($n = 6$). *b*, protein content of factors involved in mitochondrial biogenesis in AMPKγ3$^{-/-}$ mice ($n = 8$) and WT littermates ($n = 8$). *c*, representative immunoblots for the different proteins represented in Fig. 1*b*. *d*, mitochondrial content in gastrocnemius muscle from AMPKγ3$^{-/-}$ mice ($n = 7$) and homozygous WT littermates ($n = 6$). Mitochondrial content was estimated as the ratio between copy numbers of mtDNA (cytochrome b) *versus* nuclear DNA (β-actin). *e*, representative SDH staining of transversal sections of white gastrocnemius muscle from AMPKγ3$^{-/-}$ mice ($n = 4$) and homozygous WT littermates ($n = 4$). Data are represented as mean ± S.E. -fold change with respect to the corresponding homozygous WT littermates. *Open bar*, homozygous WT; *closed bar*, AMPKγ3$^{-/-}$. *, $p < 0.05$; significantly different from homozygous WT mice.

Skeletal Muscle Mitochondrial Content Is Unaltered in AMPKγ3$^{-/-}$ Mice—To determine whether the AMPK γ3 subunit was required for resting skeletal muscle mitochondrial biogenesis, we measured mRNA expression and protein content of mitochondrial markers as well as mitochondrial number in AMPKγ3$^{-/-}$ mice. mRNA content of different co-activators, transcription factors, mitochondrial markers, and lipoprotein lipase, a marker of fatty acid metabolism, were unaltered between AMPKγ3$^{-/-}$ mice and wild-type littermates. Protein contents of PGC-1α and several mitochondrial markers were unaltered between AMPKγ3$^{-/-}$ and wild-type littermates. Moreover, mitochondrial content and SDH staining were similar between AMPKγ3$^{-/-}$ and wild-type littermates (Fig. 2, *d* and *e*).

Skeletal Muscle Mitochondrial Biogenesis Is Increased in Tg-AMPKγ3^{225Q} Mice—To determine whether mutations in the AMPK γ3 subunit increase mitochondrial biogenesis in resting skeletal muscle, we studied sedentary mice overexpressing a mutant form of the AMPK γ3 subunit in glycolytic muscle (Tg-AMPKγ3^{225Q}) and analyzed mRNA expression, protein content, and mitochondrial number in skeletal muscle. We assessed mRNA content of different co-activators and transcription factors involved in the regulation of the mitochondrial biogenic process. PGC-1α, NRF-1, NRF-2, and TFAM mRNA content were significantly increased in Tg-AMPKγ3^{225Q} mice compared with nontransgenic littermates (Fig. 3*a*). mRNA of several members of the fatty acid oxidative pathway and other mitochondrial markers were increased in white gastrocnemius muscle from Tg-AMPKγ3^{225Q} mice compared with nontransgenic littermates (Fig. 3*a*). Protein content of PGC-1α, markers of the different complexes of the respiratory chain, UCP3, and PDK4 were increased in gastrocnemius muscles from Tg-AMPKγ3^{225Q} mice compared with nontransgenic littermates (Fig. 3, *b* and *c*). In contrast, protein expression of the ATP synthase subunit α was unaltered between Tg-AMPKγ3^{225Q} and nontransgenic mice. Mitochondrial content, as estimated by the relative content of mitochondrial DNA compared with nuclear DNA, was increased in Tg-AMPKγ3^{225Q} mice compared with nontransgenic littermates (Fig. 3*d*). SDH staining, a marker of the oxidative profile of individual fibers, was also increased in transversal sections of white gastrocnemius muscle from Tg-AMPKγ3^{225Q} mice (Fig. 3*e*), consistent with the increase in mitochondrial content.

Fiber Type Composition Is Unchanged in Tg-AMPKγ3^{225Q} Mice—We next assessed whether the increase in mitochondrial content in Tg-AMPKγ3^{225Q} mice is due to alterations in the skeletal muscle fiber type composition. Quantification of ATPase enzyme activity by a histological approach revealed that the percentage of type I, IIa, and IIb fibers in EDL, soleus (Fig. 4, *a* and *b*), plantaris, and gastrocnemius (not shown) was unaltered between Tg-AMPKγ3^{225Q} mice and nontransgenic littermates. Immunocytochemical staining with antibodies against type I and type IIa fibers reveals a similar pattern (Fig. 4*c*). mRNA expression of MyHC I, IIa, IIb, and IIx was unaltered between the genotypes, and quantification of the same isoforms following electrophoretic separation by glycerol-based SDS-PAGE confirmed this finding at the protein level (Fig. 4, *d* and *e*). These results provide evidence to suggest that the enhanced

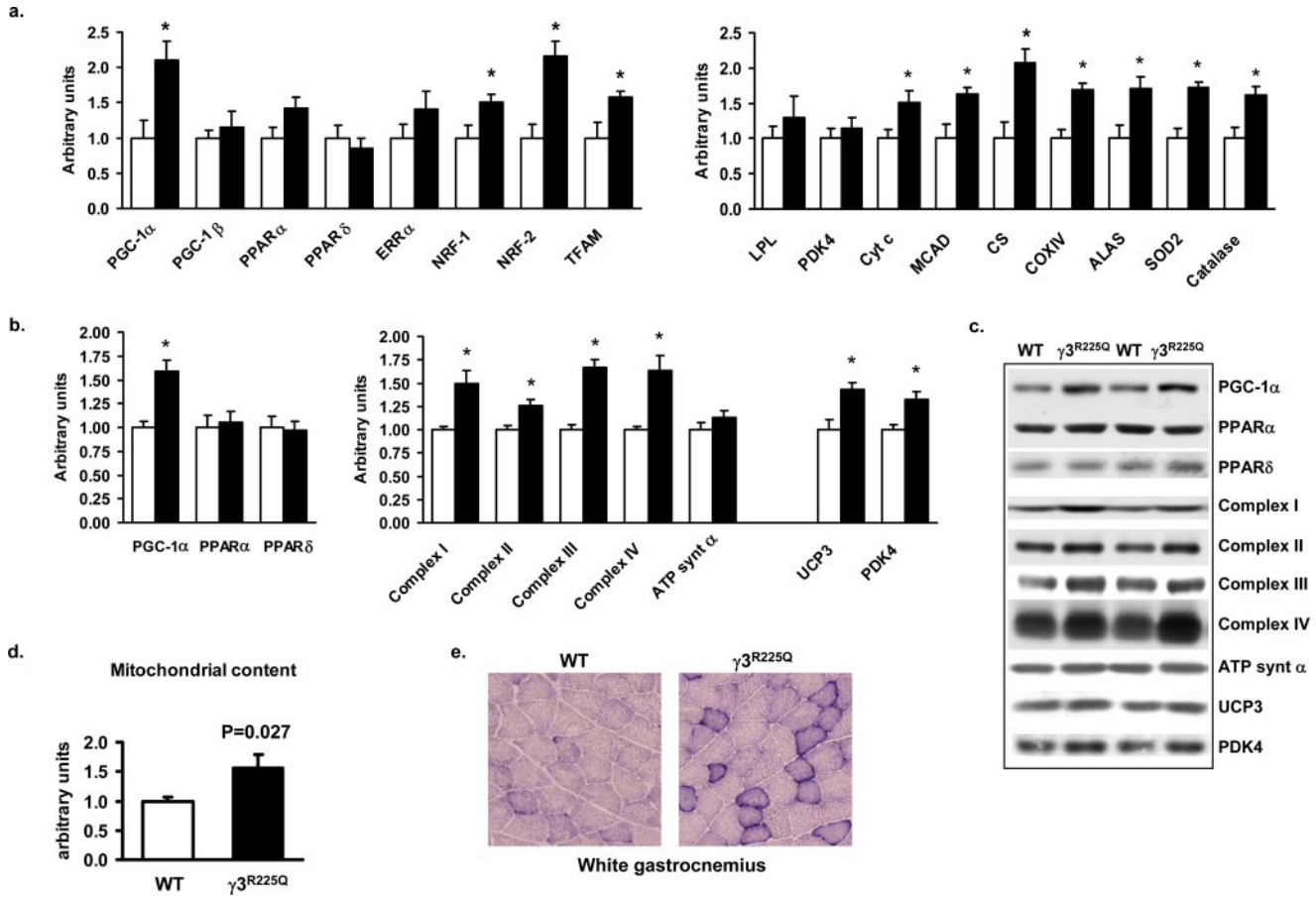

FIGURE 3. **Skeletal muscle mitochondrial biogenesis is increased in Tg-AMPKγ3^{225Q} mice.** *a*, mRNA content of different transcription factors responsible for mitochondrial biogenesis regulation and different mitochondrial markers in Tg-AMPKγ3^{225Q} mice ($n = 9$) and nontransgenic (WT) littermates ($n = 7$). *b*, protein content of mitochondrial biogenesis markers in Tg-AMPKγ3^{225Q} mice ($n = 8$) and nontransgenic littermates ($n = 8$). *c*, representative immunoblots for the different proteins represented in Fig. 1*b*. *d*, mitochondrial content in gastrocnemius muscle from Tg-AMPKγ3^{225Q} mice ($n = 6$) and nontransgenic littermates ($n = 7$). Mitochondrial content was estimated as the ratio between copy numbers of mtDNA (cytochrome *b*) *versus* nuclear DNA (β-actin). *e*, representative SDH activity of transversal sections of white gastrocnemius muscle from Tg-AMPKγ3^{225Q} mice ($n = 4$) and nontransgenic littermates ($n = 4$). Data are represented as mean ± S.E. -fold change with respect to the corresponding nontransgenic WT littermates. Nontransgenic WT (*open bar*) and Tg-AMPKγ3^{225Q} (*closed bar*). *, $p < 0.05$; significantly different from nontransgenic WT mice.

mitochondrial biogenesis and metabolic adaptations in glycolytic skeletal muscle of Tg-AMPKγ3^{225Q} mice are unrelated to fiber type reprogramming.

Skeletal Muscle Mitochondrial Total Area Is Increased in Tg-AMPKγ3^{225Q} Mice—To further characterize mitochondrial adaptations in Tg-AMPKγ3^{225Q} mice, we performed an ultrastructural examination of white gastrocnemius muscle by electron microscopy (Fig. 5*a*). Total mitochondrial area was normalized by the total area of each image and analyzed in >30 images per genotype. A total of 700–900 mitochondria were evaluated for each genotype. Mitochondrial area per total area was 54% higher in Tg-AMPKγ3^{225Q} mice *versus* nontransgenic littermates (Fig. 5*b*). The increase in mitochondrial area could be due to a higher mitochondrial density (number of mitochondria) and/or an increase in the size of the mitochondria. Features of mitochondrial dynamics, as assessed by the analysis of the electron microscopic images, were observed in intermyofibrilar mitochondria of Tg-AMPKγ3^{225Q} mice. We analyzed more than 175 mitochondrial aggregations per genotype (Fig. 5, *c* and *d*). These observations are compatible with the increased expression of different markers of mitochondrial dynamics, including fusion, fission, and degradation in gastrocnemius muscles from Tg-AMPKγ3^{225Q} mice compared with nontransgenic littermates. MFN-2 (mitofusin 2), OPA-1 (dynamin-like GTPase-optic atrophy 1), DRP-1 (dynamin-related protein 1), and LonP (Lon protease) mRNA content was increased in Tg-AMPKγ3^{225Q} mice compared with nontransgenic littermates (Fig. 5*e*). The increases in mRNA levels of fusion, fission, and degradation proteins are similar to the changes observed in other mitochondrial proteins and therefore might reflect the increased mitochondrial mass.

Skeletal Muscle Mitochondrial Respiratory Control Is Unaltered in Tg-AMPKγ3^{225Q} Mice—We next assessed mitochondrial function in permeabilized skeletal muscle fibers from Tg-AMPKγ3^{225Q} mice using high resolution respirometry to measure electron transfer and respiratory control through complex I (by adding malate, glutamate, and pyruvate) and/or complex II (by supplying succinate). Excess ADP was added to assess electron transfer coupled to oxidative phosphorylation. The mitochondrial uncoupler carbonylcyanide-4-(trifluoromethoxy)-phenylhydrazone was added to reach maximal capacity of the electron transfer system. Oxygen flux normalized to skeletal muscle weight and mitochondrial content was similar between Tg-AMPKγ3^{225Q} mice and nontransgenic lit-

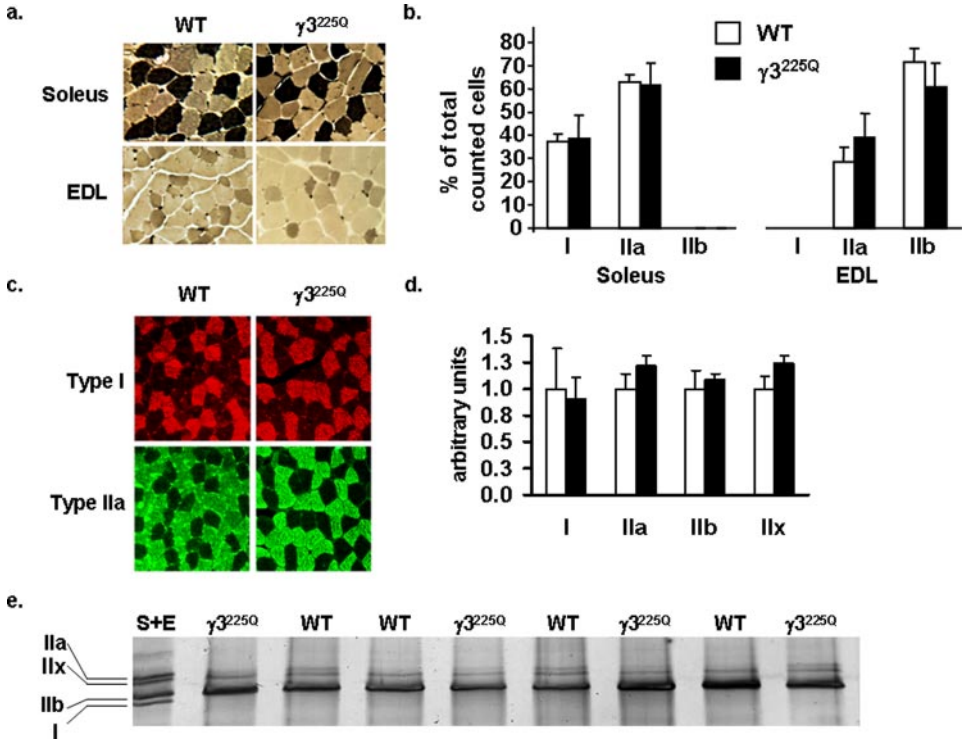

FIGURE 4. **Fiber type composition is unchanged in Tg-AMPKγ3^{225Q} mice.** *a*, representative pictures from cross-sectional areas of soleus and EDL muscles from Tg-AMPKγ3^{225Q} mice ($n = 4$) and nontransgenic WT littermates ($n = 5$) for fiber type analysis, MyoATPase staining, pH 4.45. *b*, quantification of skeletal muscle fiber types in soleus and EDL muscles based on MyoATPase staining, pH 4.45. *c*, representative image from cross-sectional areas of soleus muscle from Tg-AMPKγ3^{225Q} mice ($n = 4$) and nontransgenic WT littermates ($n = 5$) mice after immunocytochemical staining with antibodies against type I (D5) and type IIa (SC71) fibers. *d*, MyHC isoforms mRNA content in white gastrocnemius muscle from Tg-AMPKγ3^{225Q} mice ($n = 9$) and nontransgenic WT littermates ($n = 7$). *e*, representative silver staining of the different MyHC isoforms after electrophoretic separation by glycerol-based SDS-PAGE in white gastrocnemius muscle from Tg-AMPKγ3^{225Q} mice and nontransgenic WT littermates. The *first lane* from the *right* is an experimental control showing different MyHC isoform (types I, IIb, IIx, and IIa) in a pooled sample of soleus and EDL muscle homogenates ($S + E$). Data are represented as mean ± S.E. -fold change with respect to the corresponding nontransgenic WT littermates. *Open bar*, nontransgenic WT; *closed bar*, Tg-AMPKγ3^{225Q}.

termates (Fig. 6, *a* and *b*). Our results provide evidence to suggest that mitochondrial performance is similar between Tg-AMPKγ3^{225Q} mice and nontransgenic littermates.

DISCUSSION

Here we show that a single nucleotide mutation (R225Q) in the AMPK γ3 subunit is associated with mitochondrial biogenesis in glycolytic skeletal muscle, concomitant with increased expression of the co-activator PGC-1α and several transcription factors that regulate the expression of the different mitochondrial proteins. Overexpression or ablation of the AMPK γ3 subunit does not appear to play a critical role in defining skeletal muscle mitochondrial content in resting skeletal muscle, indicating that mutations in the AMPK γ3 subunit, rather than changes in subunit expression, lead to mitochondrial adaptations, possibly due to conformational transformations that facilitate AMPK function (25, 26). Most of the mutations described for the AMPK γ regulatory subunits are located near cystathionine *b*-synthase motifs that generate two Bateman domains (27) and generally interfere with the normal activation of AMPK by AMP (26). The R225Q mutant form of the AMPK γ3 subunit increases AMPK phosphorylation in transfected COS cells (17) and confers metabolic adaptations in resting glycolytic skeletal muscle that mimic endurance exercise training (15, 16).

In Hampshire pigs, a naturally occurring dominant mutation (R200Q) was identified in the AMPK γ3 regulatory subunit that is associated with increased skeletal muscle glycogen content (28). Functional analysis performed in skeletal muscle-specific transgenic mice expressing the mouse equivalent (R225Q) mutation in the AMPK γ3 subunit (Tg-AMPKγ3^{225Q} mice) reveal that this mutation increases skeletal muscle glycogen content (17, 18) and provides protection from diet-induced insulin resistance due to increased lipid oxidation (17). The increase in skeletal muscle glycogen in Tg-AMPKγ3^{225Q} mice is positively correlated with work performance, indicating enhanced ergogenics (15). Our current findings of increased skeletal muscle mitochondrial content in Tg-AMPKγ3^{225Q} mice provide a molecular basis for the increased lipid oxidation and prevention of diet-induced insulin resistance (17).

Imprinted and specialized metabolic characteristics of skeletal muscle fibers are established during differentiation (29). The mechanism by which skeletal muscle fiber differentiation leads to distinctive metabolic phenotypes, as well as the ability of mature muscle fibers to adapt to changes in energy demand, is complex and incompletely resolved. Mitochondrial adaptations in skeletal muscle can arise due to changes in specific genes (30–33). Molecular approaches using transgenic technology reveal that mice expressing an activated calcineurin under control of the muscle creatine kinase enhancer exhibit an increase in oxidative (slow twitch) skeletal muscle fibers (30) and mitochondrial biogenesis (33). Overexpression of either the co-activator PGC-1α or an activated form of the nuclear receptor PPARδ also leads to similar changes in mitochondrial biogenesis and the oxidative capacity of skeletal muscle, primarily due to a fiber type transformation from glycolytic to oxidative fibers (31, 32). However, in adult skeletal muscle, evidence supporting skeletal muscle fiber type transformation, from glycolytic type II to oxidative type I, in response to physiological perturbations, such as exercise training, is lacking, since the greatest plasticity in the exercise response is in the metabolic and enzymatic properties of the fiber rather than the twitch potential (34, 35). In humans, extreme ultraendurance exercise has little effect on fiber type composition despite improvements in oxidative enzymes (36). Even in extreme cases, such as cross-country ski training, where

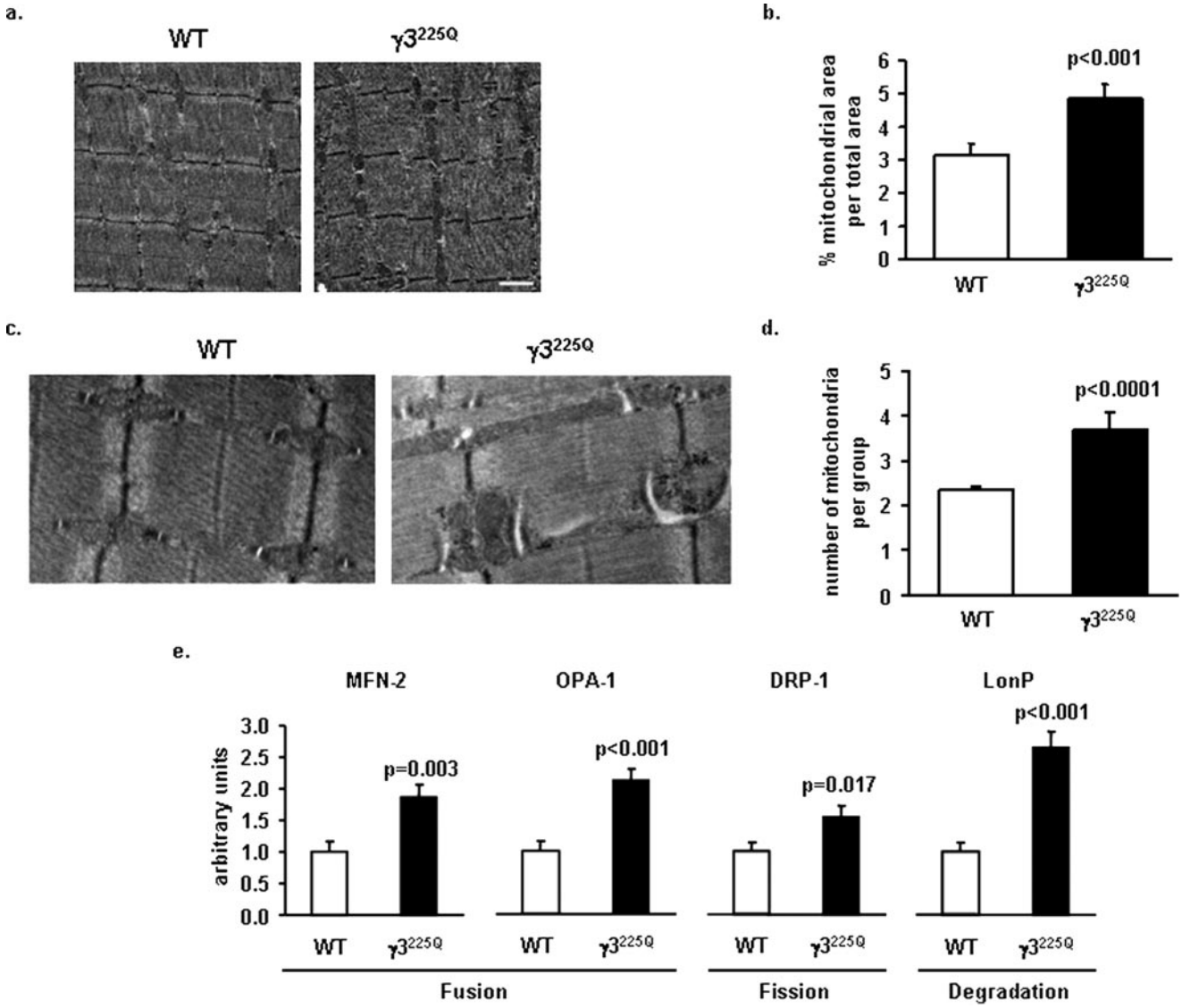

FIGURE 5. **Mitochondrial area is increased in Tg-AMPKγ3^{225Q} mice.** Mitochondrial ultrastructure was examined in white gastrocnemius muscle from Tg-AMPKγ3^{225Q} mice ($n = 4$) and nontransgenic WT littermates ($n = 4$) by transmission electron microscopy. *a*, representative micrographs from muscle specimens obtained from Tg-AMPKγ3^{225Q} and nontransgenic WT mice. *Scale bar*, 1 μM. *b*, percentage area of mitochondria was determined from images captured at ×20,400 with an area of 7.2 μm^2. *Bars*, mean ± S.E. of all images counted from 30–40 individual images (total number of mitochondria measured 700–900) per mouse strain. Area data are expressed in mitochondrial area per total image area. *c*, note that the mitochondria located between contractile units in Tg-AMPKγ3^{225Q} mice provide evidence of mitochondrial dynamics (larger mitochondria and aggregation of a higher number of mitochondria). *d*, quantification of mitochondrial aggregation as estimated by assessing more than 175 mitochondrial groups from white gastrocnemius muscle of Tg-AMPKγ3^{225Q} mice and nontransgenic WT mice. *e*, mRNA content of key regulators of mitochondrial dynamics (fusion: mitofusin 2 (*MFN-2*) and dynamin-like GTPase-optic atrophy 1 (*OPA-1*); fission: dynamin-related protein 1 (*DRP-1*); and degradation: Lon protease (*LonP*) in Tg-AMPKγ3^{225Q} mice and nontransgenic WT littermates. Data are presented as mean ± S.E.

athletes also carry a backpack and pull a sledge 18.5 miles per day for 6 days per week for 8 weeks, changes in muscle fiber type cannot fully account for the increased skeletal muscle oxidative capacity and mitochondria biogenesis (37, 38). Thus, when one considers the physiological response to exercise, which primarily involves changes in oxidative enzymes and mitochondrial biogenesis *versus* many of the transgenic and knock-out mouse models where fiber type changes arise presumably from developmental changes that reprogram the muscle phenotype, we believe that the AMPK activation in this model may mimic the physiological response to exercise. In this regard, the skeletal muscle adaptations conferred by the R225Q mutant form of the AMPK γ3 subunit phenocopy the adaptive response to exercise in humans, since changes in mitochondrial biogenesis was observed independent of fiber type transformation. Different regulatory processes could modify the imprinted characteristics and adaptability of skeletal muscle fibers during developmental stages and in the adult state.

Mitochondrial adaptations in skeletal muscle can arise due to AMPK genetic modifications in the α or γ subunit (39–42). Reductions in AMPK α2 activity due to aging are coupled to reduced mitochondrial function, insulin resistance, and Type 2 diabetes (39). Moreover, mitochondrial protein expression in resting AMPK α2 knock-out mice is reduced in skeletal muscle (40), concomitant with a decrease in the maximal mitochondrial respiration in the heart (41). Similarly, PGC-1α protein

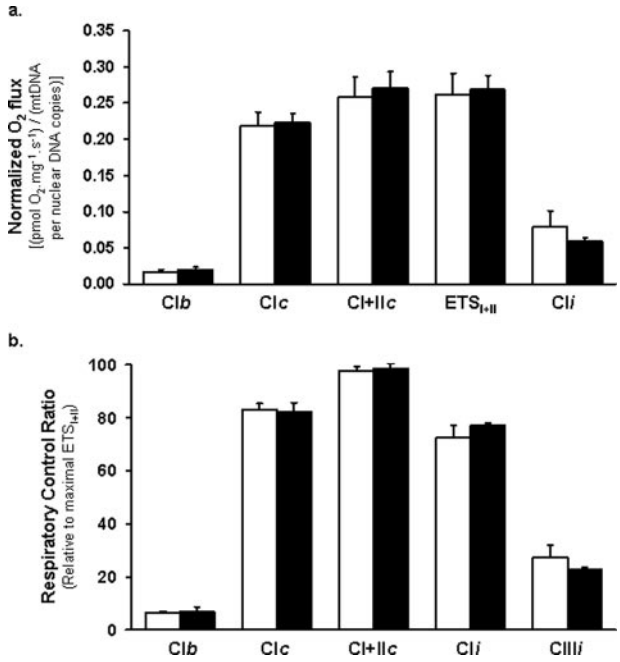

FIGURE 6. **Skeletal muscle mitochondrial respiratory control is unaltered in Tg-AMPKγ3^{225Q} mice.** Mitochondrial respiration was analyzed in permeabilized white gastrocnemius muscle samples and normalized by mitochondrial content. *a*, for basal (*b*) O_2 flux from complex I (*CI*) of the respiratory chain malate, glutamate, and pyruvate was added to the Oxygraph-2k chamber (*CIb*). To maximize oxidative phosphorylation from complex I, ADP was added in sufficient amounts to couple (*c*) electron transfer to ATP production (*CIc*). To assess the combined oxidative phosphorylation activity (maximum coupled respiration) of complex I and II, succinate was added (*CI + IIc*). To reach maximal capacity of the electron transfer system (ETS_{I+II}) by Complex I and II, an uncoupler was added (protonophore carbonylcyanide-4-(trifluoromethoxy)-phenylhydrazone). Electron transport through complex I and II was inhibited (*i*) by the sequential addition of rotenone (*CIi*) and antimycin A, respectively. The remaining O_2 flux after inhibition of complex I and III by rotenone and antimycin A (O_2 flux independent of the electron transfer system) was subtracted from each of the previous steps. Mitochondrial content was estimated as the ratio between copy numbers of mtDNA (cytochrome *b*) *versus* nuclear DNA (*β*-actin). *b*, respiratory control ratios, O_2 fluxes (*CIb*, *CIc*, *CI + IIc*, *CIi*, and *CIIIi*) normalized to electron transport system capacity (ETS_{I+II}). Data are presented as mean ± S.E. for 16–20 myofiber preparations from 8–10 mice per genotype. Shown are WT (*white columns*) and Tg-AMPKγ3^{225Q} (*black columns*) mice.

content and citrate synthase activity is reduced in skeletal muscle-specific transgenic mice expressing the inactivating D157A mutation in the AMPK α2 subunit (42). Thus, AMPK α2 isoform expression and total AMPK activity is important for mitochondrial protein expression and the oxidative capacity. Conversely mitochondrial content is unaltered in AMPKγ3$^{-/-}$ or Tg-AMPKγ3^{wt} mice, indicating that the γ3 isoform does not play a direct role.

Changes in AMPK activity conferred by the R225Q mutant in the γ3 subunit are likely to account for increased mitochondrial biogenesis. Consistent with this, PGC-1α protein content and citrate synthase activity are increased in skeletal muscle-specific transgenic mice expressing the activating R70Q mutation in the AMPK γ1 subunit (42). In contrast to the Tg-AMPKγ3^{225Q} mice, the proportion of glycolytic type IIa/x fibers is increased in AMPK γ1^{R70Q} mice, compared with wild-type littermates (42). These studies highlight the role of AMPK in the regulation of mitochondrial content and function in skeletal muscle. Polymorphisms in the AMPK γ3 subunit in humans do not seem to have an effect on glucose metabolism, but two recently identified single nucleotide polymorphisms (rs692243 and rs6436094) may play an important role in lipoprotein metabolism (43). In humans, a homologous mutation (AMPK γ3^{R225W}) increases AMPK activity and skeletal muscle glycogen content, with a concomitant decrease in intramuscular triglyceride content (44). Collectively, these studies reveal that distinct phenotypic adaptations are conferred by specific AMPK subunits. The variation observed among the different genetic modifications of AMPK subunits emphasizes the importance of defining specialized roles of the different AMPK subunit isoforms.

There are several potential mechanisms by which the R225Q mutation in the AMPK γ3 isoform can influence mitochondrial biogenesis. The AMPK γ3 isoform can form heterotrimers with the AMPK α2 and β2 subunits in glycolytic skeletal muscle (45). AMPK activation increases mitochondrial enzymes in skeletal muscle (3) by an AMPK α2-subunit dependent mechanism (40). The AMPK α2 subunit and, presumably, heterotrimers containing this subunit can be localized to the nucleus and therefore can potentially directly phosphorylate transcription factors to regulate gene expression (46). AMPK binds to and activates PGC-1α in skeletal muscle by direct phosphorylation on two critical residues, threonine 177 and serine 538 (7), providing a potential mechanism for the effects of the mutation on skeletal mitochondrial biogenesis. AMPK appears to require PGC-1α for effects on GLUT4 and mitochondrial gene expression in skeletal muscle (7). The mutations may modify the nuclear localization of AMPK or the interaction with PGC-1α. Clearly, the mutated form of the AMPK γ3 subunit leads to transcriptional changes that influence the oxidative capacity of skeletal muscle fibers through increased mitochondrial biogenesis.

The mechanism for the increase in mitochondria biogenesis in the Tg-AMPKγ3^{225Q} mice may involve increased DNA binding of transcription factors, such as MEF (myocyte enhancer factor). MEF2A, the predominant MEF2 gene product expressed in postnatal cardiac muscle, plays a specific role in maintaining appropriate mitochondrial content and cytoarchitectural integrity (47). MEF2 interacts with the co-activator PGC-1α (48) and NRF-1 to provide a mechanism for mitochondrial biogenesis regulation (49). In skeletal muscle, various factors, including insulin, hydrogen peroxide, osmotic stress, contraction, and 5-aminoimidazole-4-carboxamide-1-β-D-ribofuranoside, acutely increase MEF2 DNA binding (50, 51), implicating insulin- and AMPK-dependent signaling pathways as playing a role. Compound C, an AMPK inhibitor, prevents the acute 5-aminoimidazole-4-carboxamide-1-β-D-ribofuranoside-induced as well as contraction-induced MEF2 DNA binding in skeletal muscle (50), providing pharmacological evidence that action of AMPK is linked to MEF2 DNA binding. These studies provide evidence that the effects of 5-aminoimidazole-4-carboxamide-1-β-D-ribofuranoside and contraction on MEF2 DNA binding are rapid and cannot be attributed to changes in muscle fiber type composition. Thus, we cannot exclude the possibility that AMPK-induced increases in MEF2 DNA binding increase mitochondrial biogenesis in Tg-AMPKγ3^{225Q} mice. However, AMPK-activated increases in MEF2 DNA binding have also been linked to GLUT4 biogen-

esis (50–54), but given that GLUT4 protein expression is unaltered in Tg-AMPK$\gamma3^{225Q}$ mice,[3] an alternative mechanism for the increase in mitochondria biogenesis warrants further consideration. Our results suggest that the R225Q mutation in the AMPK γ3 promotes changes in signal transduction that increase expression, and possibly activity, of PGC-1α and several transcription factors that regulate mitochondrial biogenesis, including NRF-1, NRF-2, and TFAM.

In conclusion, the R225Q mutation in the AMPK γ3 subunit induces mitochondrial biogenesis in glycolytic skeletal muscle independent of changes in fiber type composition. The relevance of this modification in the AMPK γ3 isoform in glycolytic skeletal muscle fibers highlights the potential role for AMPK to modulate metabolic responses that influence whole body metabolism. Pharmacological perturbation of the AMPK γ3 isoform could be relevant for the treatment of metabolic diseases.

Acknowledgments—We thank Professor Stefano Schiaffino for providing the D5 and SC-71 antibodies and for expert advice on skeletal muscle histochemistry. We also thank Professor Barbara Canlon for access to equipment for the histochemical analysis, Professor Oleg Supliakov for guidance with the electron microscope, and Professor Erich Gnaiger for advice on mitochondrial respiration.

REFERENCES

1. Holloszy, J. O. (1967) *J. Biol. Chem.* **242,** 2278–2282
2. Kelly, D. P., and Scarpulla, R. C. (2004) *Genes Dev.* **18,** 357–368
3. Winder, W. W., Holmes, B. F., Rubink, D. S., Jensen, E. B., Chen, M., and Holloszy, J. O. (2000) *J. Appl. Physiol.* **88,** 2219–2226
4. Bergeron, R., Ren, J. M., Cadman, K. S., Moore, I. K., Perret, P., Pypaert, M., Young, L. H., Semenkovich, C. F., and Shulman, G. I. (2001) *Am. J. Physiol.* **281,** E1340–E1346
5. Zong, H., Ren, J. M., Young, L. H., Pypaert, M., Mu, J., Birnbaum, M. J., and Shulman, G. I. (2002) *Proc. Natl. Acad. Sci. U. S. A.* **99,** 15983–15987
6. Putman, C. T., Kiricsi, M., Pearcey, J., MacLean, I. M., Bamford, J. A., Murdoch, G. K., Dixon, W. T., and Pette, D. (2003) *J. Physiol.* **551,** 169–178
7. Jager, S., Handschin, C., St.-Pierre, J., and Spiegelman, B. M. (2007) *Proc. Natl. Acad. Sci. U. S. A.*, 0705070104
8. Aguilar, V., Alliouachene, S., Sotiropoulos, A., Sobering, A., Athea, Y., Djouadi, F., Miraux, S., Thiaudière, E., Foretz, M., Viollet, B., Diolez, P., Bastin, J., Benit, P., Rustin, P., Carling, D., Sandri, M., Ventura-Clapier, R., and Pende, M. (2007) *Cell Metab.* **5,** 476–487
9. Ruderman, N., and Prentki, M. (2004) *Nat. Rev. Drug Discov.* **3,** 340–351
10. Kahn, B. B., Alquier, T., Carling, D., and Hardie, D. G. (2005) *Cell Metab.* **1,** 15–25
11. Long, Y. C., and Zierath, J. R. (2006) *J. Clin. Invest.* **116,** 1776–1783
12. Wojtaszewski, J. F. P., Birk, J. B., Frosig, C., Holten, M., Pilegaard, H., and Dela, F. (2005) *J. Physiol.* **564,** 563–573
13. Gao, G., Fernandez, C. S., Stapleton, D., Auster, A. S., Widmer, J., Dyck, J. R. B., Kemp, B. E., and Witters, L. A. (1996) *J. Biol. Chem.* **271,** 8675–8681
14. Hoppeler, H., and Fluck, M. (2003) *Med. Sci. Sports Exerc.* **35,** 95–104
15. Barnes, B. R., Glund, S., Long, Y. C., Hjalm, G., Andersson, L., and Zierath, J. R. (2005) *FASEB J.* **19,** 773–779
16. Barnes, B. R., Long, Y. C., Steiler, T. L., Leng, Y., Galuska, D., Wojtaszewski, J. F. P., Andersson, L., and Zierath, J. R. (2005) *Diabetes* **54,** 3484–3489
17. Barnes, B. R., Marklund, S., Steiler, T. L., Walter, M., Hjalm, G., Amarger, V., Mahlapuu, M., Leng, Y., Johansson, C., Galuska, D., Lindgren, K., Abrink, M., Stapleton, D., Zierath, J. R., and Andersson, L. (2004) *J. Biol. Chem.* **279,** 38441–38447
18. Long, Y., Barnes, B., Mahlapuu, M., Steiler, T., Martinsson, S., Leng, Y., Wallberg-Henriksson, H., Andersson, L., and Zierath, J. (2005) *Diabetologia* **48,** 2354
19. Mahlapuu, M., Johansson, C., Lindgren, K., Hjalm, G., Barnes, B. R., Krook, A., Zierath, J. R., Andersson, L., and Marklund, S. (2004) *Am. J. Physiol.* **286,** E194–E200
20. Nilsson, E. C., Long, Y. C., Martinsson, S., Glund, S., Garcia-Roves, P., Svensson, L. T., Andersson, L., Zierath, J. R., and Mahlapuu, M. (2006) *J. Biol. Chem.* **281,** 7244–7252
21. Schiaffino, S., and Bormioli, S. P. (1973) *J. Histochem. Cytochem.* **21,** 142–145
22. Talmadge, R. J., and Roy, R. R. (1993) *J. Appl. Physiol.* **75,** 2337–2340
23. Kuznetsov, A. V., Schneeberger, S., Seiler, R., Brandacher, G., Mark, W., Steurer, W., Saks, V., Usson, Y., Margreiter, R., and Gnaiger, E. (2004) *Am. J. Physiol.* **286,** H1633–H1641
24. Boushel, R., Gnaiger, E., Schjerling, P., Skovbro, M., Kraunsøe, R., and Dela, F. (2007) *Diabetologia* **50,** 790–796
25. Scott, J. W., Hawley, S. A., Green, K. A., Anis, M., Stewart, G., Scullion, G. A., Norman, D. G., and Hardie, D. G. (2004) *J. Clin. Invest.* **113,** 274–284
26. Sanders, M. J., Grondin, P. O., Hegarty, B. D., Snowden, M. A., and Carling, D. (2007) *Biochem. J.* **403,** 139–148
27. Xiao, B., Heath, R., Saiu, P., Leiper, F. C., Leone, P., Jing, C., Walker, P. A., Haire, L., Eccleston, J. F., Davis, C. T., Martin, S. R., Carling, D., and Gamblin, S. J. (2007) *Nature* **449,** 496–500
28. Milan, D., Jeon, J.-T., Looft, C., Amarger, V., Robic, A., Thelander, M., Rogel-Gaillard, C., Paul, S., Iannuccelli, N., Rask, L., Ronne, H., Lundstr, ouml, m, K., Reinsch, N., Gellin, J., Kalm, E., Roy, P. L., Chardon, P., and Andersson, L. (2000) *Science* **288,** 1248–1251
29. Hodgson, J. A., Roy, R. R., Higuchi, N., Monti, R. J., Zhong, H., Grossman, E., and Edgerton, V. R. (2005) *J. Exp. Biol.* **208,** 3761–3770
30. Naya, F. J., Mercer, B., Shelton, J., Richardson, J. A., Williams, R. S., and Olson, E. N. (2000) *J. Biol. Chem.* **275,** 4545–4548
31. Lin, J., Wu, H., Tarr, P. T., Zhang, C.-Y., Wu, Z., Boss, O., Michael, L. F., Puigserver, P., Isotani, E., Olson, E. N., Lowell, B. B., Bassel-Duby, R., and Spiegelman, B. M. (2002) *Nature* **418,** 797
32. Wang, Y.-X., Zhang, C.-L., Yu, R. T., Cho, H. K., Nelson, M. C., Bayuga-Ocampo, C. R., Ham, J., Kang, H., and Evans, R. M. (2004) *PLoS Biol.* **2,** e294
33. Long, Y. C., Glund, S., Garcia-Roves, P. M., and Zierath, J. R. (2007) *J. Biol. Chem.* **282,** 1607–1614
34. Booth, F. W., and Thomason, D. B. (1991) *Physiol. Rev.* **71,** 541–585
35. Fitts, R. H. (2003) *Am. J. Phys. Med. Rehabil.* **82,** 320–331
36. Zierath, J. R., and Hawley, J. A. (2004) *PLoS Biol.* **2,** e348
37. Schantz, P., Billeter, R., Henriksson, J., and Jansson, E. (1982) *Muscle Nerve* **5,** 628–636
38. Schantz, P., Henriksson, J., and Jansson, E. (1983) *Clin. Physiol.* **3,** 141–151
39. Reznick, R. M., Zong, H., Li, J., Morino, K., Moore, I. K., Yu, H. J., Liu, Z. X., Dong, J., Mustard, K. J., Hawley, S. A., Befroy, D., Pypaert, M., Hardie, D. G., Young, L. H., and Shulman, G. I. (2007) *Cell Metab.* **5,** 151–156
40. Jorgensen, S. B., Treebak, J. T., Viollet, B., Schjerling, P., Vaulont, S., Wojtaszewski, J. F., and Richter, E. A. (2007) *Am. J. Physiol.* **292,** E331–E339
41. Athea, Y., Viollet, B., Mateo, P., Rousseau, D., Novotova, M., Garnier, A., Vaulont, S., Wilding, J. R., Grynberg, A., Veksler, V., Hoerter, J., and Ventura-Clapier, R. (2007) *Diabetes* **56,** 786–794
42. Rockl, K. S. C., Hirshman, M. F., Brandauer, J., Fujii, N., Witters, L. A., and Goodyear, L. J. (2007) *Diabetes* **56,** 2062–2069
43. Weyrich, P., Machicao, F., Staiger, H., Simon, P., Thamer, C., Machann, J., Schick, F., Guirguis, A., Fritsche, A., Stefan, N., and Häring, H. U. (2007) *Diabetologia* **50,** 2097–2106
44. Costford, S. R., Kavaslar, N., McPherson, R., and Harper, M.-E. (2007) *PLoS ONE* **2,** e903

[3] P. M. Garcia-Roves, M. E. Osler, M. H. Holmström, and J. R. Zierath, unpublished observation.

45. Birk, J. B., and Wojtaszewski, J. F. P. (2006) *J. Physiol.* (*Lond.*) **577,** 1021–1032
46. Leff, T. (2003) *Biochem. Soc. Trans.* **31,** 224–227
47. Naya, F. J., Black, B. L., Wu, H., Bassel-Duby, R., Richardson, J. A., Hill, J. A., and Olson, E. N. (2002) *Nat. Med.* **8,** 1303–1309
48. Handschin, C., Rhee, J., Lin, J., Tarr, P. T., and Spiegelman, B. M. (2003) *Proc. Natl. Acad. Sci. U. S. A.* **100,** 7111–7116
49. Ramachandran, B., Yu, G., and Gulick, T. (2008) *J. Biol. Chem.* **283,** 11935–11946
50. Al-Khalili, L., Chibalin, A. V., Yu, M., Sjodin, B., Nylen, C., Zierath, J. R., and Krook, A. (2004) *Am. J. Physiol.* **286,** C1410–C1416
51. Song, X. M., Fiedler, M., Galuska, D., Ryder, J. W., Fernstrom, M., Chibalin, A. V., Wallberg-Henriksson, H., and Zierath, J. R. (2002) *Diabetologia* **45,** 56–65
52. Holmes, B. F., Sparling, D. P., Olson, A. L., Winder, W. W., and Dohm, G. L. (2005) *Am. J. Physiol.* **289,** E1071–E1076
53. Ju, J. S., Smith, J. L., Oppelt, P. J., and Fisher, J. S. (2005) *Am. J. Physiol.* **288,** E347–E352
54. Ojuka, E. O., Jones, T. E., Han, D.-H., Chen, M., Wamhoff, B. R., Sturek, M., and Holloszy, J. O. (2002) *Am. J. Physiol.* **283,** E1040–E1045